Electronic Supplementary Information (ESI)

Octanuclear Ni(II) cubes based on halogen-substituted pyrazolates: Synthesis, structure, electrochemistry and magnetism

Zhi Wang,[a] Zvonko Jagličić,[b] Lu-Lu Han,[a] Gui-Lin Zhuang,[c] Geng-Geng Luo[d] Su-Yuan Zeng,[e] Chen-Ho Tung,[a] and Di Sun*,[a]

[a]*Key Lab of Colloid and Interface Chemistry, Ministry of Education, School of Chemistry and Chemical Engineering, Shandong University, Jinan, 250100, P. R. China. E-mail: dsun@sdu.edu.cn*

[b]*Faculty of Civil and Geodetic Engineering & Institute of Mathematics, Physics and Mechanics, University of Ljubljana, Jamova 2, 1000 Ljubljana, Slovenia.*

[c]*College of Chemical Engineering and Materials Science, Zhejiang University of Technology, Hangzhou, 310032, People's Republic of China.*

[d]*College of Materials Science and Engineering, Huaqiao University, Xiamen 361021, People's Republic of China.*

[e]*School of Chemistry and Chemical Engineering, Liaocheng University, Liaocheng, People's Republic of China.*

Table S1. Selected bond lengths and angles for 1-3.

Complex 1			
Ni1—N2^{i}	2.028 (3)	O1—Ni1^{iii}	2.166 (2)
Ni1—N3	2.029 (3)	O1—Ni1^{iv}	2.182 (2)
Ni1—N1	2.045 (3)	O1—Ni1^{v}	2.182 (2)
Ni1—O1	2.166 (2)	O2—Ni1^{i}	2.1842 (13)
Ni1—O1^{ii}	2.182 (2)	O2—Ni1^{vi}	2.1842 (12)
Ni1—O2	2.1842 (12)	O2—Ni1^{iv}	2.1842 (13)
Ni1—Ni1^{iii}	2.9799 (11)	N2—Ni1^{iv}	2.028 (3)
N2^{i}—Ni1—N3	94.88 (12)	N1—Ni1—O1^{ii}	169.85 (13)
N2^{i}—Ni1—N1	96.38 (12)	O1—Ni1—O1^{ii}	81.48 (15)
N3—Ni1—N1	96.22 (12)	N2^{i}—Ni1—O2	90.61 (12)
N2^{i}—Ni1—O1	169.60 (13)	N3—Ni1—O2	169.98 (15)
N3—Ni1—O1	92.02 (12)	N1—Ni1—O2	91.48 (12)
N1—Ni1—O1	90.59 (12)	O1—Ni1—O2	81.48 (13)
N2^{i}—Ni1—O1^{ii}	90.68 (12)	O1^{ii}—Ni1—O2	81.12 (13)
N3—Ni1—O1^{ii}	90.42 (12)		
Symmetry codes: (i) *y*, −*x*+1, *z*; (ii) *y*, −*x*+1, −*z*+1; (iii) *x*, *y*, −*z*+1; (iv) −*y*+1, *x*, *z*; (v) −*y*+1, *x*, −*z*+1; (vi) −*x*+1, −*y*+1, *z*.			
Complex 2			
Ni1—N2	2.018 (12)	Ni3—N13	2.030 (13)
Ni1—N11	2.040 (11)	Ni3—O3i	2.145 (9)
Ni1—N1	2.042 (10)	Ni3—O1	2.165 (9)
Ni1—O2i	2.161 (8)	Ni3—O3	2.173 (9)
Ni1—O2	2.163 (8)	Ni3—Ni3i	2.976 (4)
Ni1—O1	2.219 (9)	Ni3—Ni4	2.977 (3)
Ni1—Ni1i	2.958 (3)	Ni4—N7	1.989 (11)
Ni1—Ni4	2.973 (2)	Ni4—N10	2.027 (12)
Ni1—Ni2	2.989 (2)	Ni4—N8	2.034 (13)
Ni2—N9i	2.007 (11)	Ni4—O2	2.138 (8)
Ni2—N3	2.026 (11)	Ni4—O1	2.151 (9)
Ni2—N4	2.027 (12)	Ni4—O3	2.170 (9)
Ni2—O1	2.152 (9)	Ni4—Ni2i	2.975 (3)
Ni2—O3i	2.169 (9)	O2—Ni1i	2.161 (8)
Ni2—O2i	2.169 (8)	O2—Ni2i	2.169 (8)
Ni2—Ni4i	2.975 (3)	O3—Ni3i	2.145 (9)
Ni2—Ni3	2.979 (3)	O3—Ni2i	2.169 (9)
Ni3—N5	2.009 (12)	N9—Ni2i	2.007 (11)
Ni3—N6	2.009 (11)		

N2—Ni1—N11	95.0 (4)	N5—Ni3—N6	98.3 (5)
N2—Ni1—N1	94.3 (5)	N5—Ni3—N13	97.4 (6)
N11—Ni1—N1	97.2 (4)	N6—Ni3—N13	93.7 (5)
N2—Ni1—O2i	90.9 (4)	N5—Ni3—O3i	93.2 (4)
N11—Ni1—O2i	168.4 (4)	N6—Ni3—O3i	167.5 (4)
N1—Ni1—O2i	92.3 (4)	N13—Ni3—O3i	89.5 (4)
N2—Ni1—O2	169.5 (4)	N5—Ni3—O1	88.4 (4)
N11—Ni1—O2	92.5 (4)	N6—Ni3—O1	94.3 (4)
N1—Ni1—O2	92.1 (3)	N13—Ni3—O1	169.3 (4)
O2i—Ni1—O2	80.5 (3)	O3i—Ni3—O1	81.2 (3)
N2—Ni1—O1	92.0 (4)	N5—Ni3—O3	168.9 (4)
N11—Ni1—O1	89.3 (4)	N6—Ni3—O3	87.2 (4)
N1—Ni1—O1	170.5 (4)	N13—Ni3—O3	91.8 (5)
O2i—Ni1—O1	80.5 (3)	O3i—Ni3—O3	80.6 (4)
O2—Ni1—O1	80.6 (3)	O1—Ni3—O3	81.5 (3)
N9i—Ni2—N3	95.6 (5)	N7—Ni4—N10	95.6 (5)
N9i—Ni2—N4	97.4 (5)	N7—Ni4—N8	94.5 (5)
N3—Ni2—N4	96.1 (5)	N10—Ni4—N8	96.1 (5)
N9i—Ni2—O1	169.3 (4)	N7—Ni4—O2	169.5 (4)
N3—Ni2—O1	90.3 (4)	N10—Ni4—O2	93.6 (4)
N4—Ni2—O1	90.8 (4)	N8—Ni4—O2	89.7 (4)
N9i—Ni2—O3i	92.3 (4)	N7—Ni4—O1	92.3 (4)
N3—Ni2—O3i	169.8 (4)	N10—Ni4—O1	88.1 (4)
N4—Ni2—O3i	89.3 (4)	N8—Ni4—O1	171.6 (4)
O1—Ni2—O3i	80.9 (3)	O2—Ni4—O1	82.7 (3)
N9i—Ni2—O2i	89.0 (4)	N7—Ni4—O3	88.5 (4)
N3—Ni2—O2i	92.6 (4)	N10—Ni4—O3	169.4 (4)
N4—Ni2—O2i	168.5 (5)	N8—Ni4—O3	93.3 (5)
O1—Ni2—O2i	81.8 (3)	O2—Ni4—O3	81.7 (3)
O3i—Ni2—O2i	81.0 (3)	O1—Ni4—O3	81.9 (3)
Symmetry code: (i) −x+1, y, −z+1/2.			
Complex 3			
Ni1—N3	2.002 (15)	Ni3—N6	2.046 (19)
Ni1—N7i	2.026 (15)	Ni3—O2	2.104 (13)
Ni1—N2	2.028 (17)	Ni3—O1i	2.128 (15)
Ni1—O3i	2.185 (13)	Ni3—O3	2.147 (12)
Ni1—O2	2.229 (13)	Ni3—Ni1i	2.992 (4)
Ni1—O1	2.234 (14)	Ni4—N10	1.988 (18)
Ni1—Ni2	2.953 (4)	Ni4—N8	2.024 (15)
Ni1—Ni4i	2.987 (3)	Ni4—N11	2.041 (15)
Ni1—Ni3i	2.992 (4)	Ni4—O2i	2.179 (15)
Ni2—N9	1.967 (16)	Ni4—O1	2.181 (15)
Ni2—N4	2.036 (16)	Ni4—O3	2.195 (13)

Ni2—N5	2.05 (2)	Ni4—Ni1i	2.987 (3)
Ni2—O2	2.130 (15)	O1—Ni3i	2.128 (15)
Ni2—O3	2.147 (12)	O2—Ni4i	2.179 (15)
Ni2—O1	2.167 (14)	O3—Ni1i	2.185 (13)
Ni2—Ni4	2.978 (4)	N1—Ni3i	1.960 (19)
Ni3—N1i	1.960 (19)	N7—Ni1i	2.026 (15)
Ni3—N12i	2.020 (15)	N12—Ni3i	2.020 (15)
N3—Ni1—N7i	94.1 (7)	N1i—Ni3—N6	97.5 (8)
N3—Ni1—N2	94.3 (7)	N12i—Ni3—N6	99.0 (7)
N7i—Ni1—N2	99.2 (7)	N1i—Ni3—O2	168.6 (7)
N3—Ni1—O3i	167.6 (7)	N12i—Ni3—O2	89.7 (6)
N7i—Ni1—O3i	92.4 (5)	N6—Ni3—O2	91.8 (7)
N2—Ni1—O3i	95.1 (6)	N1i—Ni3—O1i	88.7 (7)
N3—Ni1—O2	89.6 (6)	N12i—Ni3—O1i	89.1 (6)
N7i—Ni1—O2	93.5 (6)	N6—Ni3—O1i	169.2 (6)
N2—Ni1—O2	166.4 (7)	O2—Ni3—O1i	81.1 (5)
O3i—Ni1—O2	79.4 (5)	N1i—Ni3—O3	94.2 (7)
N3—Ni1—O1	93.0 (6)	N12i—Ni3—O3	167.4 (6)
N7i—Ni1—O1	170.7 (5)	N6—Ni3—O3	87.9 (6)
N2—Ni1—O1	86.3 (6)	O2—Ni3—O3	79.5 (5)
O3i—Ni1—O1	79.6 (5)	O1i—Ni3—O3	82.9 (5)
O2—Ni1—O1	80.5 (5)	N1i—Ni3—Ni1i	66.3 (6)
N9—Ni2—N4	96.0 (7)	N10—Ni4—N8	97.1 (7)
N9—Ni2—N5	93.3 (7)	N10—Ni4—N11	98.8 (6)
N4—Ni2—N5	96.2 (7)	N8—Ni4—N11	94.7 (6)
N9—Ni2—O2	168.8 (6)	N10—Ni4—O2i	165.6 (6)
N4—Ni2—O2	93.1 (6)	N8—Ni4—O2i	94.0 (6)
N5—Ni2—O2	92.2 (6)	N11—Ni4—O2i	89.4 (5)
N9—Ni2—O3	91.5 (6)	N10—Ni4—O1	89.7 (6)
N4—Ni2—O3	171.2 (6)	N8—Ni4—O1	170.9 (5)
N5—Ni2—O3	87.9 (6)	N11—Ni4—O1	90.1 (5)
O2—Ni2—O3	78.9 (5)	O2i—Ni4—O1	78.3 (5)
N9—Ni2—O1	88.7 (6)	N10—Ni4—O3	90.0 (6)
N4—Ni2—O1	93.0 (6)	N8—Ni4—O3	92.7 (5)
N5—Ni2—O1	170.4 (6)	N11—Ni4—O3	167.7 (5)
O2—Ni2—O1	84.3 (5)	O2i—Ni4—O3	80.3 (5)
O3—Ni2—O1	82.6 (5)	O1—Ni4—O3	81.2 (4)
N1i—Ni3—N12i	95.3 (7)		
Symmetry code: (i) −x, −y, −z.			

Figure S1. The XRD patterns of 1-3.

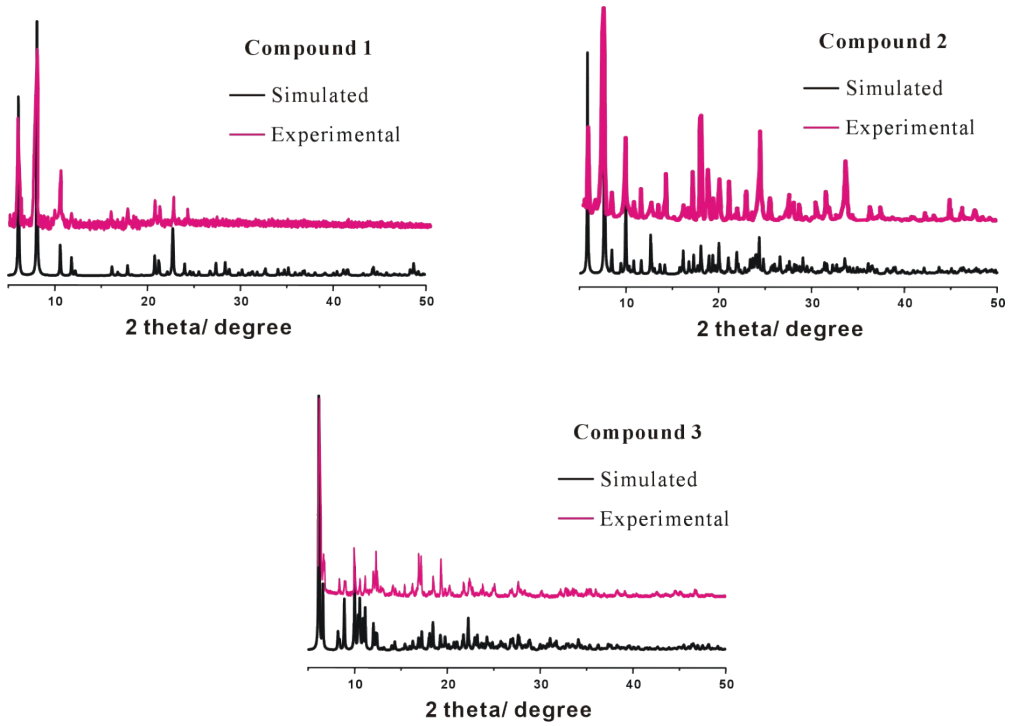

As shown in Fig. S1, the X-ray powder diffraction patterns measured for the as-synthesized samples are in good agreement with the PXRD patterns simulated from the respective single-crystal X-ray data, proving the purity of the bulk phases. The dissimilarity in reflection intensities between the simulated and the experimental patterns may be due to the different orientation of the microcrystals in the powder samples.

Figure S2. The TGA plots for 1-3.

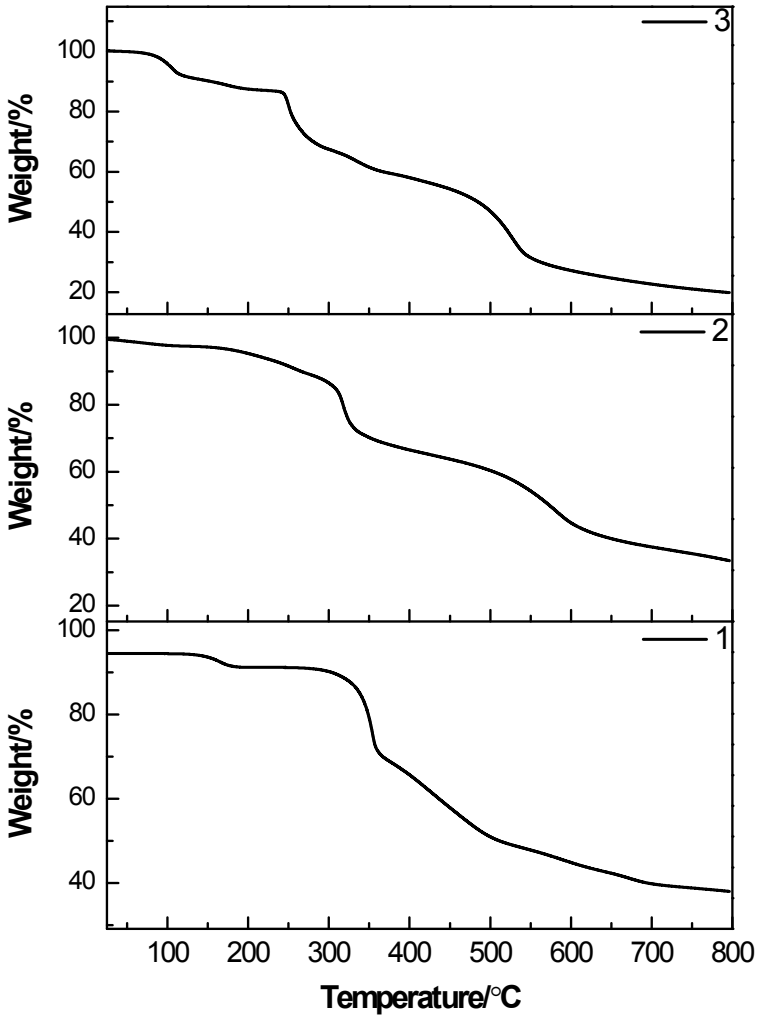

The thermal properties of **1-3** were examined by thermogravimetric analysis (TGA) under nitrogen atmosphere. It is clearly observed from the TG-curve: The first weight loss (3.5%) of compound **1** in the range of 130-184 ^{o}C corresponds to the loss of two MeCN molecules (cal. 3.8%). For compound **2**, two MeCN molecules were lost when the temperature up to 150 ^{o}C (obs. 3.0 %; cal. 3.1%). The TG curve of compound **3** showed gradual weight loss of 14.0 % from 80-238 ^{o}C which matches the removal of twelve MeCN molecules (cal. 13.5%).

Figure S3. The IR for 1-3.

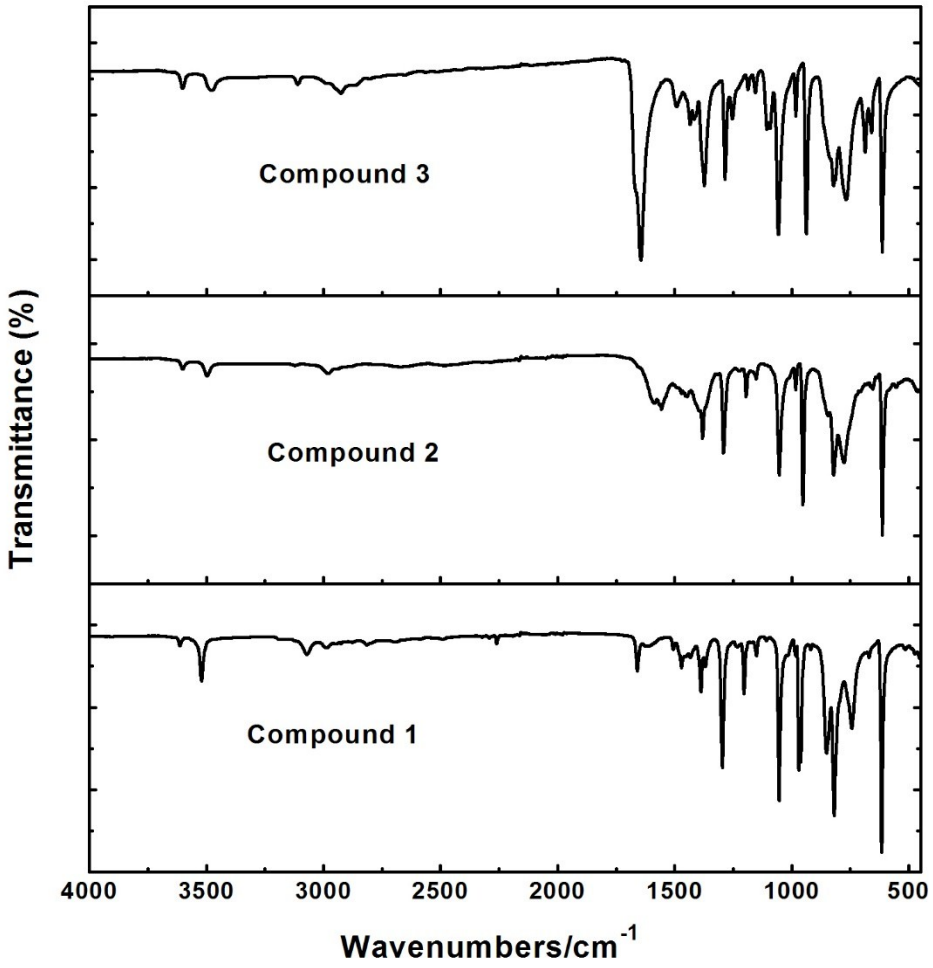

IR characterization

The infrared spectra of compound **1** to **3** are very similar to each other. The peaks in the range of 3400 to 3600 cm^{-1} are assigned to the O-H stretching vibration of hydroxyl, in the region from 2900 to 3100 cm^{-1} are attributed to the C-H stretching vibration of quaternary ammonium salt and Xpz ligands, in the range of 1550 to 1662 cm^{-1} belong to the C=C and C=N stretching vibration of Xpz ligands, in the region of 1365 to 1400 cm^{-1} are attributed to the C-H bending vibration of quaternary ammonium salt and Xpz ligands, in the region of 1250 to 940 cm^{-1} are assigned to the molecular skeleton of vibration, and at the range of 850 to 500 cm^{-1} belong to the vibration of C-X of Xpz ligands. (X = Cl, Br and I).

Figure S4. CVs of 1- (a), 2- (b), and 3-CPEs (c).

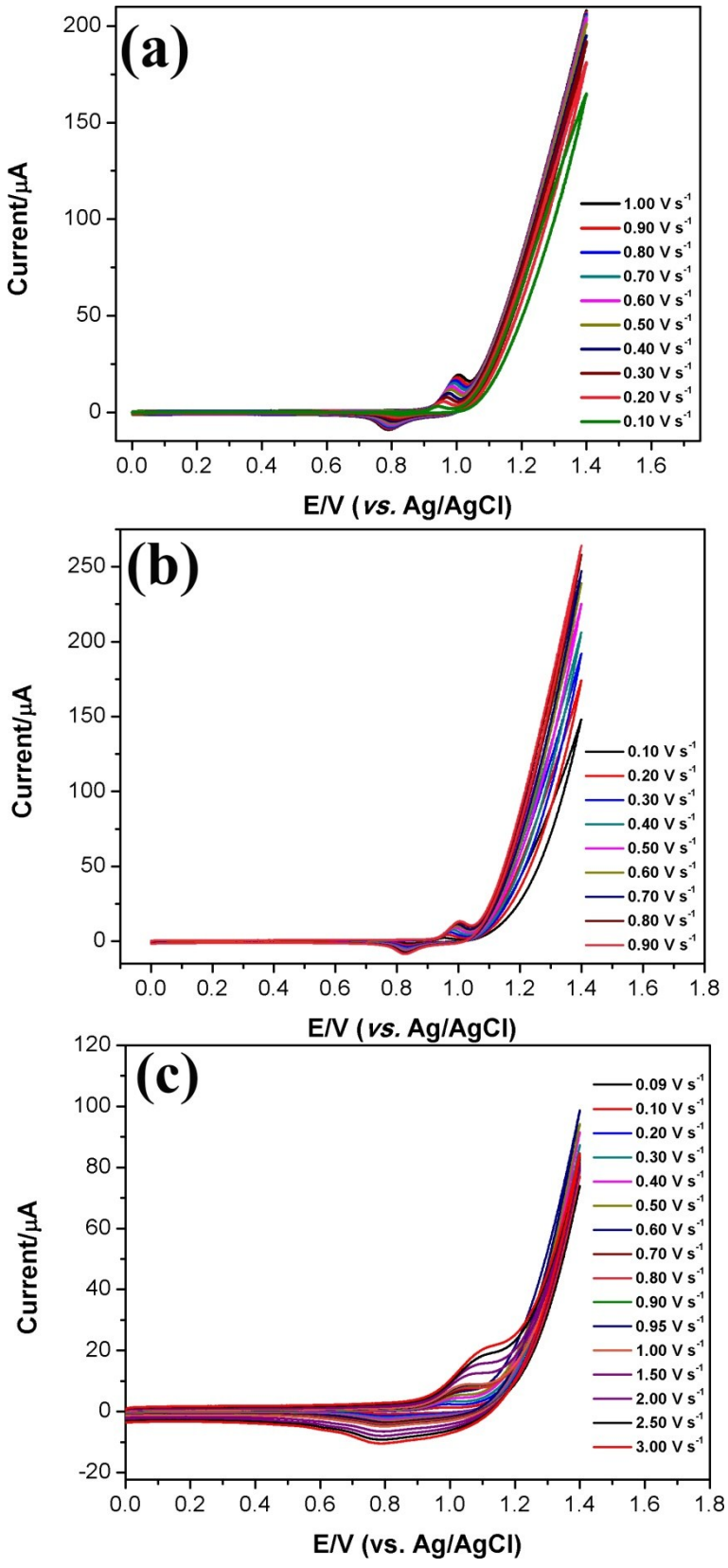

Figure S5. 50 consecutive CV cycles of 1-, 2-, and 3-GCEs at 200 mV s^{-1}.

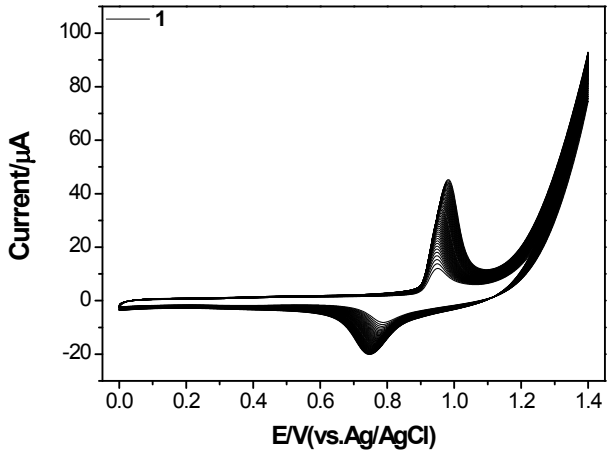

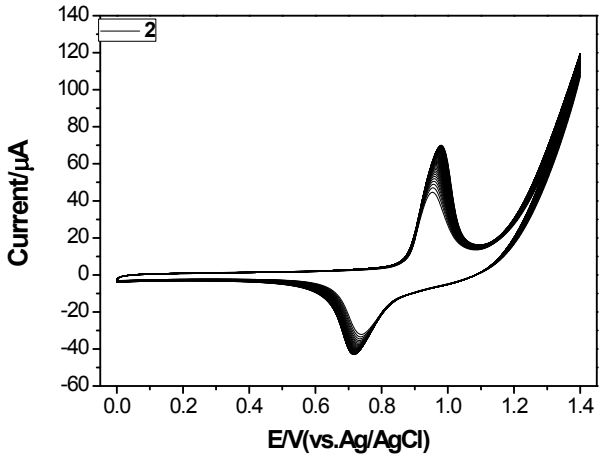

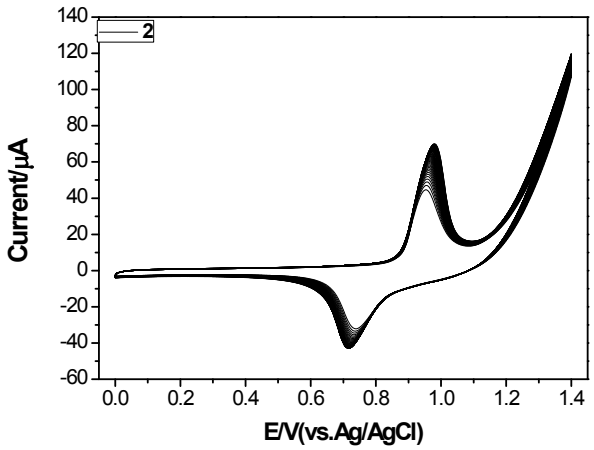

Figure S6 Frontier orbitals of 1: HOMO-1(a), HOMO (b), LUMO(c) and LUMO+1(d)

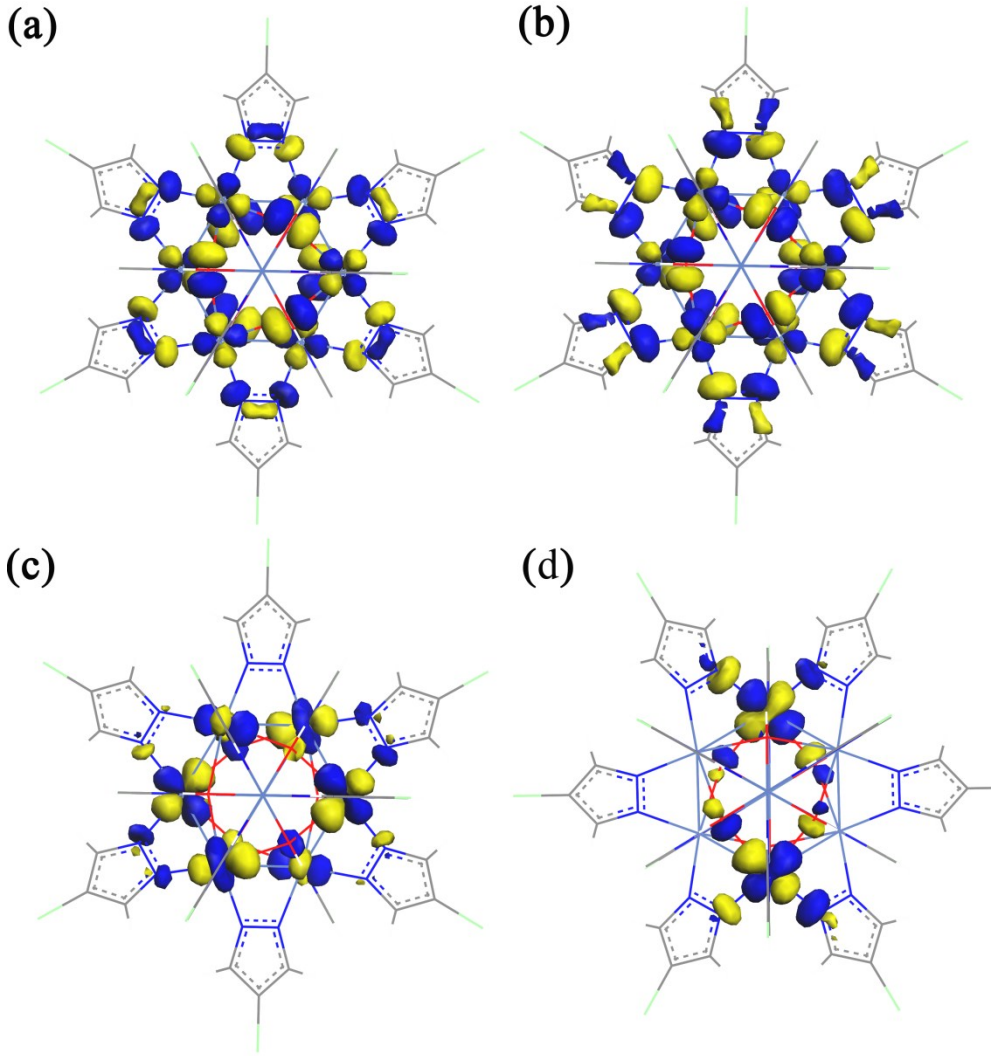

Computational Detail:

All DFT calculations were carried out in the DMol3 module [1] of Material Studio software. The exchange-correlation (XC) effects are described by using of Revised PBE functional by Hammer et al [2] with generalized gradient approximation (GGA) [2] Effective Core Potentials (ECP) approach was used to treat the inner electrons of Co atom, and $3d^8 4s^2$ electrons of Ni atom were explicitly treated as valence electrons. The double numerical basis set plus polarization functional (DNP) [3], which has a computational precision, being comparable to the split-valence basis set 6-31g**, was applied in the expanded electronic wave function. For the calculations, the optimization convergence in energy and force was set to be 1.0×10^{-5} Ha and 2.0×10^{-3} Ha. $Å^{-1}$, and the SCF convergence was set to be 1.0×10^{-6}.

Reference:

1. (a) B. Delley, *J. Chem. Phys.*, 1990, **92**, 508; (b) B. Delley, *The Journal of Chemical Physics*, 1991, **94**, 7245; (c) B. Delley, *J. Chem. Phys.*, 2000, **113**, 7756.

2. Hammer, B.; Hansen, L. B.; Norskov, J. K. Phys. Rev. B, 1999, 59, 7413.

3. J. P. Perdew, K. Burke and M. Ernzerhof, *Phys. Rev. Lett.*, 1996, **77**, 3865.